doi:10.1093/brain/awaa223 BRAIN 2020: 143; 2803–2817 | 2803

BRAIN
A JOURNAL OF NEUROLOGY

Phosphorylated tau interactome in the human Alzheimer's disease brain

Eleanor Drummond,[1,2,*] Geoffrey Pires,[2,3,*] Claire MacMurray,[2] Manor Askenazi,[4] Shruti Nayak,[5] Marie Bourdon,[2] Jiri Safar,[6,7] Beatrix Ueberheide[4,8] and Thomas Wisniewski[2,9]

*These authors contributed equally to this work.

Accumulation of phosphorylated tau is a key pathological feature of Alzheimer's disease. Phosphorylated tau accumulation causes synaptic impairment, neuronal dysfunction and formation of neurofibrillary tangles. The pathological actions of phosphorylated tau are mediated by surrounding neuronal proteins; however, a comprehensive understanding of the proteins that phosphorylated tau interacts with in Alzheimer's disease is surprisingly limited. Therefore, the aim of this study was to determine the phosphorylated tau interactome. To this end, we used two complementary proteomics approaches: (i) quantitative proteomics was performed on neurofibrillary tangles microdissected from patients with advanced Alzheimer's disease; and (ii) affinity purification-mass spectrometry was used to identify which of these proteins specifically bound to phosphorylated tau. We identified 542 proteins in neurofibrillary tangles. This included the abundant detection of many proteins known to be present in neurofibrillary tangles such as tau, ubiquitin, neurofilament proteins and apolipoprotein E. Affinity purification-mass spectrometry confirmed that 75 proteins present in neurofibrillary tangles interacted with PHF1-immunoreactive phosphorylated tau. Twenty-nine of these proteins have been previously associated with phosphorylated tau, therefore validating our proteomic approach. More importantly, 34 proteins had previously been associated with total tau, but not yet linked directly to phosphorylated tau (e.g. synaptic protein VAMP2, vacuolar-ATPase subunit ATP6V0D1); therefore, we provide new evidence that they directly interact with phosphorylated tau in Alzheimer's disease. In addition, we also identified 12 novel proteins, not previously known to be physiologically or pathologically associated with tau (e.g. RNA binding protein HNRNPA1). Network analysis showed that the phosphorylated tau interactome was enriched in proteins involved in the protein ubiquitination pathway and phagosome maturation. Importantly, we were able to pinpoint specific proteins that phosphorylated tau interacts with in these pathways for the first time, therefore providing novel potential pathogenic mechanisms that can be explored in future studies. Combined, our results reveal new potential drug targets for the treatment of tauopathies and provide insight into how phosphorylated tau mediates its toxicity in Alzheimer's disease.

1 Brain and Mind Centre and Central Clinical School, Faculty of Medicine and Health, University of Sydney, Australia
2 Centre for Cognitive Neurology, Department of Neurology, New York University School of Medicine, New York, NY, USA
3 Alzheimer's and Prion Diseases Team, Paris Brain Institute, CNRS, UMR 7225, INSERM 1127, Sorbonne University UM75, Paris, France
4 Biomedical Hosting LLC, USA
5 Proteomics Laboratory, Division of Advanced Research Technologies, NYU School of Medicine, New York, NY, USA
6 Department of Pathology, Case Western Reserve University, Cleveland, OH, USA
7 Department of Neurology, Case Western Reserve University, Cleveland, OH, USA
8 Department of Biochemistry and Molecular Pharmacology, New York University School of Medicine, New York, NY, USA
9 Department of Psychiatry, New York University School of Medicine, New York, NY, USA

Received December 18, 2019. Revised May 5, 2020. Accepted May 22, 2020. Advance access publication August 19, 2020

Correspondence to: Eleanor Drummond
Brain and Mind Centre, 94 Mallett Street, Camperdown, NSW, Australia, 2050
E-mail: Eleanor.drummond@sydney.edu.au

Correspondence may also be addressed to: Thomas Wisniewski
Centre for Cognitive Neurology, Department of Neurology, New York University School of Medicine,
New York, NY, USA
E-mail: Thomas.Wisniewski@nyulangone.org

Keywords: Alzheimer's disease; tau; phosphorylation; proteomics; neurofibrillary tangles

Abbreviations: AP-MS = affinity purification-mass spectrometry; co-IP = co-immunoprecipitation; NFT = neurofibrillary tangle; pTau = phosphorylated tau

Introduction

Neurofibrillary tangles (NFTs) are one of the key pathological hallmarks of Alzheimer's disease. NFTs primarily consist of phosphorylated tau (pTau). In the healthy brain tau binds to microtubules, providing stability and facilitating axonal transport (Mandelkow and Mandelkow, 2012; Sotiropoulos *et al.*, 2017). However, in Alzheimer's disease tau becomes hyperphosphorylated, causing it to disassociate from microtubules and aggregate into the paired helical filaments that are present in NFTs and dystrophic neurites (Spillantini and Goedert, 2013). This accumulation of pTau is associated with synaptic impairment, neurodegeneration and the development of dementia. How pTau specifically mediates these toxic effects is still unknown.

Determining the proteins that pathological pTau interacts with in Alzheimer's disease would increase our understanding of how pTau is involved in the pathogenesis of Alzheimer's disease and could lead to the discovery of new drug targets. Currently, our knowledge of the proteins that pTau interacts with in the human Alzheimer's disease brain is surprisingly limited. To date, three previous studies have used affinity purification-mass spectrometry (AP-MS) to identify the binding partners of total tau in human Alzheimer's disease brain tissue (Meier *et al.*, 2015; Ayyadevara *et al.*, 2016; Hsieh *et al.*, 2019). However, it is currently still unknown which of these proteins specifically interact with the more pathologically relevant pTau species. Previous targeted studies have shown that the interaction between tau and surrounding neuronal proteins is crucial for regulating its role in disease. For example, the physiological interaction between tau and microtubules is thought to prevent abnormal aggregation of tau in the healthy brain (Kellogg *et al.*, 2018). Interaction between tau and select kinases (CDK5, CAMK2A, GSK3β) results in phosphorylation, dissociation from microtubules and aggregation of tau (Baumann *et al.*, 1993; Litersky *et al.*, 1996; Lovestone *et al.*, 1996). Protein interactions also regulate pTau degradation via the ubiquitin-proteasome system or autophagy (Lee *et al.*, 2013). Specifically in Alzheimer's disease, protein interactions mediate amyloid-β-associated neurotoxicity and synaptic pathology; for example, interactions between tau, Fyn and amyloid-β mediates excitotoxicity (Ittner *et al.*, 2010) and the interaction between pTau and synaptogyrin-3 is hypothesized to regulate synaptic impairment (McInnes *et al.*, 2018). Given the pathological importance of interactions between pTau and surrounding neuronal proteins, the goal of our current study was to comprehensively identify proteins that interact with pTau in Alzheimer's disease brain tissue using unbiased proteomics approaches. In this study we used two complementary proteomic approaches (localized proteomics and AP-MS) to identify proteins present in neurons with NFTs and to identify the proteins that directly interact with pTau in the human Alzheimer's disease brain.

Materials and methods

Ethics statement

All procedures were performed under protocols approved by Institutional Review Boards at Case Western Reserve University and University Hospitals Case Medical Center in Cleveland, OH and New York University Alzheimer Disease Center, NY. In all cases, written informed consent for research was obtained from the patient or legal guardian, and the material used had appropriate ethical approval for use in this project. All patients' data and samples were coded and handled according to NIH guidelines to protect patients' identities.

Patients and clinical evaluations

Seven cases of sporadic Alzheimer's disease were included in the localized proteomics study of NFTs and five cases of sporadic Alzheimer's disease were included in the pTau interactome study. Cases were randomly selected from donated brain tissue collected at the Department of Pathology at Case Western Reserve University and at the New York University Alzheimer's Disease Clinical Center (NYU ADC). Individual patient information [sex, age, ABC neuropathological score (Montine *et al.*, 2012), and post-mortem interval time] is included in Table 1 (except for a few cases where post-mortem interval was not recorded).

Laser capture microdissection of neurofibrillary tangles

NFTs were microdissected from formalin-fixed paraffin embedded (FFPE) blocks of human brain tissue containing the hippocampus and entorhinal cortex that were collected and

Table 1 Patient characteristics

Proteomics study type	Patient ID	Sex	Age	ABC Score	PMI, h
Localized proteomics of NFTs	sAD1	Female	91	A3, B3, C3	14
	sAD2	Female	67	A3, B3, C3	67
	sAD3	Female	84	A3, B3, C2	n/a
	sAD4	Female	85	A2, B2, C1	n/a
	sAD5	Male	81	A3, B3, C3	18
	sAD6	Male	89	A3, B3, C3	n/a
	sAD7	Male	81	A3, B3, C3	20
pTau interactome	sAD8	Male	76	A3, B3, C3	12
	sAD9	Female	90	A3, B3, C3	15
	sAD10	Male	69	A3, B3, C3	6
	sAD11	Male	62	A3, B3, C3	14
	sAD12	Female	61	A3, B3, C3	8

n/a = not available; PMI = post-mortem interval.

processed as part of routine autopsy procedures. Laser capture microdissection (LCM) of NFTs was performed using our published protocol (Drummond *et al.*, 2018*b*). FFPE sections (8-µm thick) were collected onto LCM-compatible PET Frame Slides (Leica). NFTs were visualized using chromogenic immunohistochemistry using our previously described protocol (Drummond *et al.*, 2018*b*). Briefly, sections were dewaxed and rehydrated by a series of xylene and ethanol washes, sections were treated with H_2O_2 [0.3% in phosphate-buffered saline (PBS) for 20 min at room temperature] and blocking solution [10% normal goat serum (NGS) in PBS for 1 h at room temperature] and incubated with an anti-phosphorylated tau antibody (AT8; Thermo; cat. #MN1020; 1:500 diluted in 4% NGS; overnight at 4°C). Sections were then incubated with anti-mouse biotinylated IgG secondary antibody (1:1000; 2 h at room temperature), followed by ABC solution (1 h at room temperature), and finally with 3,3′-diaminobenzidene (DAB). Sections were then thoroughly rinsed with PBS and ddH_2O and allowed to completely dry prior to LCM. NFTs (1.5 mm^2 total area) were manually microdissected from each sample using a LMD6500 microscope (Leica). NFTs were selected for microdissection based the presence of AT8 staining that was present in a morphological pattern typical of NFTs. As such, proteomic results reflect proteins present in both living neurons and ghost tangles. The 1.5 mm^2 total area consisted of ∼4000 NFTs per sample. As collection of this many NFTs was not feasible to do in one sitting, three samples of 0.5 mm^2 total area were collected separately and combined prior to peptide extraction. NFTs were collected into caps containing ddH_2O. After collection, samples were centrifuged at 14 000*g* for 2 min and stored at −80°C until peptide extraction.

Localized proteomics of neurofibrillary tangles

Sample preparation

Samples were processed for label-free quantitative LC-MS/MS using our published formic acid extraction protocol (Drummond *et al.*, 2015, 2018*b*). Briefly, NFTs were resuspended in 100 mM ammonium bicarbonate/20% acetonitrile solution and deparaffinized by heating at 95°C for 1 h followed by 65°C for 2 h. Samples were dried in a SpeedVac concentrator and subsequently incubated in 70% LC-MS grade formic acid overnight at room temperature. Samples were sonicated three times for 3 min and vortexed in between sonication. Samples were dried in the SpeedVac again and next resuspended in 100 mM ammonium bicarbonate. The proteins were reduced with dithiothreitol (DTT; 20 mM) at 57°C for 1 h and alkylated with iodoacetamide (50 mM) at room temperature for 45 min. Protein samples were digested with 250 ng of sequencing grade-modified trypsin (Promega) overnight at room temperature with gentle agitation. Samples were acidified with 0.5% formic acid and 0.2% trifluoroacetic acid (TFA) and peptides were desalted using POROS beads. Briefly, a slurry of R2 20 µm POROS beads (Life Technologies Corporation) was added to each sample. Samples were incubated with agitation at 4°C for 3 h. The beads were loaded onto equilibrated C18 ziptips (Millipore) using a microcentrifuge for 30 s at 6000 rpm. POROS beads were rinsed three times with 0.1% TFA followed by microcentrifugation. Extracted porous beads were further washed with 0.5% acetic acid. Peptides were eluted off the beads by addition of 40% acetonitrile in 0.5% acetic acid followed by the addition of 80% acetonitrile in 0.5% acetic acid. The organic solvent was removed using a SpeedVac concentrator and the samples were reconstituted in 0.5% acetic acid and stored at −80°C until further analysis.

LC-MS/MS analysis

An aliquot of each sample was loaded onto a trap column (Acclaim® PepMap 100 pre-column, 75 µm × 2 cm, C18, 3 µm, 100 Å, Thermo Scientific) connected to an analytical column (EASY-Spray column, 50 m × 75 µm ID, PepMap RSLC C18, 2 µm, 100 Å, Thermo Scientific) using the autosampler of an EASY-nLC 1000 HPLC (ThermoFisher). The peptides were gradient eluted [solvent A (2% acetonitrile, 0.5% acetic acid); solvent B (95% acetonitrile, 0.5% acetic acid)] directly into a Q Exactive (Thermo Scientific) mass spectrometer using the following gradient: in 120 min from 2 to 30% solvent B, in 10 min to 40% solvent B and to 100% solvent B in another 10 min. The Q Exactive mass spectrometer acquired high-resolution full MS spectra with a resolution of 70 000, automatic gain control (AGC) target of 10^6, with a maximum ion time of 120 ms, and scan range of 400–1500 m/z. Following each full MS, 20 data-dependent high-resolution higher-energy collisional dissociation (HCD) MS/MS spectra were acquired using a resolution of 17 500, AGC target of 5×10^4, maximum ion time of 120 ms, one microscan, 2 m/z isolation window, fixed first mass of 150 m/z, normalized collision energy (NCE) of 27 and dynamic exclusion of 30 s.

LC-MS/MS data analysis

Protein quantitation was performed using the MaxQuant software suite (Cox *et al.*, 2014). The MS/MS spectra were searched against the UniProt human reference proteome database using Andromeda (Cox *et al.*, 2011) using the following settings: oxidized methionine (M) and deamidation (asparagine and glutamine) were selected as variable modifications, and carbamidomethyl (C) as fixed modifications; precursor mass tolerance was set to 10 ppm; fragment mass tolerance was set to 0.01 Th. Formalin fixation induced modifications were not included as their level was determined to be low in a mass error tolerant search using Byonic (Bern *et al.*, 2012). The identifications were filtered with a false discovery rate (FDR) of > 0.01 using a target-decoy approach at the protein and peptide level. Only protein groups with $\geqslant 2$ unique peptide identifications/protein were further analysed. Label-free quantification (LFQ)

intensity values were log2 transformed and protein group quantification was performed only for protein groups that were identified in at least three of seven cases. Missing values were imputed based on normal distribution. Keratins were removed from the analysis.

Human brain sample homogenization for phosphorylated tau AP-MS

Five cases of sporadic Alzheimer's disease were used for AP-MS studies (Table 1). Grey matter from the frontal cortex was dissected from archived fresh frozen human tissue samples that were stored at –80°C. Cortical tissue (0.25 g per sample) was homogenized using a gentle method optimized to maintain protein-protein interactions. Frozen tissue was initially pulverized using a hammer and then Dounce homogenized on ice (25 strokes) in a low salt homogenization buffer [50 mM HEPES pH 7.0, 250 mM sucrose, 1 mM EDTA, Protease inhibitor cocktail (cOmplete™ ULTRA Tablets, Mini, EDTA-free; Millipore Sigma; cat. #5892791001) and phosphatase inhibitor cocktail (PhosphoSTOP™ EASYpack; Millipore Sigma; cat. #4906845001)]. Total protein concentration of homogenates was determined using a BCA assay.

Co-immunoprecipitation for AP-MS

Mass spectrometry was used to analyse co-immunoprecipitation (co-IP) products generated using 1.5 mg total brain homogenate and 10 µg of antibody per sample. Two co-IPs were performed for each case; one using the antibody PHF1 (provided by Dr Peter Davies) to affinity enrich phosphorylated tau and its binding partners, and one using a mouse IgG isotype control antibody (BioLegend, cat. #400202) to control for non-specific binding. As a result, 10 separate co-IP samples were individually analysed using LC-MS/MS. Brain homogenate and antibody were incubated overnight at 4°C with over-end rotation to allow antibody binding. Samples were then incubated with Dynabeads (7.5 mg/sample) overnight at 4°C with over-end rotation. Antibody/Dynabead complexes were recovered using a magnet, resuspended in 100 µl elution buffer for 5 min to remove the co-IP product from the Dynabeads, and stored at –20°C until use.

Western blot

Western blot was used to confirm that the co-IP for phosphorylated tau was successful. Five per cent of the IP product was mixed in Bolt™ LDS Sample Buffer (Life Technologies) without DTT or boiling in order to preserve the aggregated structure of paired helical filaments. Proteins were resolved on 4–12% Bis-Tris gels (Life Technologies) and then transferred to 0.2 µm nitrocellulose membranes (Bio-Rad). Blots were blocked with 5% milk in Tris-buffered saline with Tween for 1 h and probed with anti-pTau (1:3000; BioLegend; cat. #SIG-39472) at room temperature for 1 h. Finally, blots were incubated with anti-rabbit horseradish peroxidase-labelled antibody (1:3000; GE Healthcare). Western blot results were visualized using enhanced chemiluminescence (Pierce ECL; Thermo Scientific; #32106). Signals were captured using ChemiDoc imaging system (Bio-Rad).

AP-MS proteomics

Sample preparation

Eluted co-IP products were reduced with DTT (20 mM) at 57°C for 1 h and alkylated with iodoacetamide (50 mM) at room temperature for 45 min, and run on a NuPAGE™ 4-12% Bis-Tris 1.0 mm Gel (Life Technologies). The gel was stained with GelCode Blue Stain Reagent (Thermo Scientific) and the IgG bands excised and analysed separately on the mass spectrometer from the rest of the gel. The excised bands were destained in a 1:1 (v/v) methanol/100 mM ammonium bicarbonate solution and dehydrated using acetonitrile followed by a SpeedVac concentrator. The dehydrated gel pieces were rehydrated with 200 ng of trypsin (Promega) in 100 mM ammonium bicarbonate enough to cover the gel pieces and allowed to digest overnight at room temperature with gentle agitation. A slurry of R2 50 µM POROS™ Beads (Thermo Scientific) in 5% formic acid, 0.2% TFA was added to the samples at a volume double of the 100 mM ammonium bicarbonate used to rehydrate the gel pieces. The samples were left to shake for 3 h at 4°C. The beads were loaded onto equilibrated C18 ZipTips® (Millipore) and desalted as described above for the localized proteomics. The desalted peptide mixture was stored at –80°C until further analysis.

LC-MS/MS analysis

An aliquot of each peptide mixture was loaded onto a trap column (Acclaim® PepMap 100 pre-column, 75 µm × 2 cm, C18, 3 µm, 100 Å, Thermo Scientific) connected to an analytical column (EASY-Spray column, 50 m × 75 µm ID, PepMap RSLC C18, 2 µm, 100 Å, Thermo Scientific) using the autosampler of an EASY-nLC 1200 HPLC (ThermoFisher). The peptides were gradient eluted [solvent A (2% acetonitrile, 0.5% acetic acid); solvent B (80% acetonitrile, 0.5% acetic acid)] directly into a Orbitrap Fusion™ Lumos (Thermo Scientific) mass spectrometer using the following gradient: 5 min at 5% solvent B, in 80 min to 25% solvent B, in 15 min to 45% solvent B and to 100% solvent B in another 10 min. High resolution full mass spectra (MS) were obtained with a resolution of 240 000, AGC target of 10^6, a maximum injection time of 50 ms, and a scan range of 400–500 m/z. Following each full MS, HCD MS/MS spectra were acquired in the ion trap (rapid scan mode) with a top N methods (3 s) using an AGC target of 2×10^4, a maximum injection time of 18 ms, one microscan, 0.7 m/z isolation window, a fixed first mass of 110 m/z, and an NCE of 30.

LC-MS/MS data analysis

The MS/MS spectra were searched against the UniProt human reference proteome database using SEQUEST within Proteome Discoverer. The search parameters were as follows: precursor mass tolerance ± 10 ppm, fragment mass tolerance ± 0.4 Da, trypsin cleavage with two missed cleavages allowed, variable modification of oxidation of methionine, phosphorylation on serine, threonine and tyrosine, and deamidation of glutamine and asparagine and fixed modification of carbamidomethylation of cysteine. Peptides and proteins were filtered to better than 1% FDR using a target-decoy database strategy and proteins required at least two unique peptides to be reported. To obtain a probabilistic score (SAINT score) that a protein is a *bona fide* pTau interactor, the data were analysed using the SAINTexpress algorithm (Choi *et al.*, 2011) at https://reprint-apms.org. The results of fold change and SAINT analysis were

plotted in a one-sided volcano plot. Proteins that had a SAINT score $\geqslant 0.65$ were considered to be potential pTau interactors and further analysed.

Localized proteomics and AP-MS bioinformatic analysis

Protein enrichment analyses were performed using Ingenuity Pathway Analysis (IPA; Qiagen) and STRING (Version 11.0) (Szklarczyk *et al.*, 2019). IPA was used to identify upstream regulator proteins, which were determined based on prior knowledge of expected effects between regulator and target proteins/genes stored in the Ingenuity Knowledge Database. This analysis determined whether proteins in NFTs were enriched for a particular upstream regulator (statistically determined using Fisher's exact test and threshold for significance set to $P < 0.01$) (Kramer *et al.*, 2014). Cell type enrichment analysis was conducted by leveraging a previously curated (as used in Drummond *et al.*, 2017) list of brain cell-type-specific genes for the following brain cell types: astrocytes, endothelial, microglia, neurons and oligodendrocytes based on data published in Zhang *et al.* (2016). The enrichment analysis consisted of a Fisher's exact test using a entire proteogenome (downloaded from UniProt on 20 May 2019) as background, where the subset observed to be enriched in pTau is compared to the subset known to be specific to every given cell-type.

Systematic literature searches were used to determine whether a protein had novel association with tau. The following PubMed searches were performed for all 125 potential pTau interactors: 'tau' and Gene ID; 'tau' and protein name; 'neurofibrillary tangle' and Gene ID; 'neurofibrillary tangle' and protein name. Gene ID or protein name aliases were also taken into account and contributed to a positive search result. A protein was designated as present in NFTs if there was published immunohistochemistry evidence of co-localization of this protein in NFTs or if it was identified in NFTs by at least two peptides in either of the two previous proteomic studies of NFTs using human brain tissue (Wang *et al.*, 2005; Minjarez *et al.*, 2013). Previously reported interaction with tau was determined by comparison with published studies of the tau interactome in mouse (Liu *et al.*, 2016; Wang *et al.*, 2017; Maziuk *et al.*, 2018) and human brains (Meier *et al.*, 2015; Ayyadevara *et al.*, 2016; Hsieh *et al.*, 2019) or by co-IP confirmation in targeted studies identified through PubMed searches. Previous association with Alzheimer's disease was determined by systematic PubMed searches for 'Alzheimer's disease' and Gene ID or 'Alzheimer's disease' and protein name, or by identification in our in-house developed database (NeuroPro), which compiles data from all previous proteomic studies that analysed human Alzheimer's disease brain samples (Andreev *et al.*, 2012; Hondius *et al.*, 2016; Seyfried *et al.*, 2017; Johnson *et al.*, 2018; Zhang *et al.*, 2018; Mendonca *et al.*, 2019; Xu *et al.*, 2019). Previous proteomic studies of Alzheimer's disease brain tissue were only included in NeuroPro if they contained data that allowed for sufficiently stringent statistical comparison between Alzheimer's disease and control samples (significance shown by either FDR-corrected *t*-test or *t*-test in combination with fold chance difference between groups >1.5). Protein identifications from these previous studies were only included if proteins were identified by at least two peptides per protein. Proteins were designated as having novel association with Alzheimer's disease if they did not have positive search results for any of the searches/comparisons described above.

Validation studies: co-immunoprecipitation

To validate interactions, immunoprecipitations of HSP90B1, SCRN1 and EZR were performed. Immunoprecipitations were performed using 300 μg of human brain homogenate from one of the cases used for AP-MS studies (Case sAD8), and 2 μg of anti-SCRN1 (LSBio; cat. #LS-C162903), anti-HSP90B1 (Sigma, cat. #HPA003901), anti-Ezrin (Thermo Scientific; clone 3C12; cat. #35-7300), rabbit IgG isotype control (Thermo Fisher Scientific, cat. #02-6102) or mouse IgG isotype control (BioLegend, cat. #400202) antibodies. Antibody and brain homogenate were incubated overnight at 4°C. Immunocomplexes were then incubated with 1.5 mg Dynabeads Protein G magnetic beads (Invitrogen; cat. #1003D) overnight at 4°C. Beads were washed four times and IP product was eluted in elution buffer (glycine pH 2.8). To confirm pTau co-IP, western blot was performed using PHF1 (Ser396/Ser404, mouse monoclonal; 1:500; P. Davies) for HSP90B1 and SCRN1 immunoprecipitations and two separate anti-phosphorylated tau antibodies for EZR immunoprecipitation (Ser404, rabbit polyclonal, 1:3000, BioLegend; cat. #SIG-39472 and Ser199/Ser202, rabbit polyclonal, 1:1500; Invitrogen; cat. #44-768G).

Data availability

The mass spectrometry raw files are accessible under MassIVE ID: MSV000085305 and ProteomeXchange ID: PXD018629.

Results

Proteome of neurofibrillary tangles in sporadic Alzheimer's disease

The first goal of our study was to determine the proteins present in NFT-containing neurons (hereafter referred to as NFTs) in advanced sporadic Alzheimer's disease. To this end, NFTs were microdissected from Alzheimer's disease brain tissue using laser capture microdissection ($n = 7$ cases). A total NFT area of 1.5 mm^2 was microdissected per case, each containing on average 3831 ± 279 tangles (average ± standard error of the mean). LC-MS was performed on each of these samples individually to determine the proteins present in NFTs. LC-MS identified 542 proteins in NFTs (Supplementary material). As expected, tau was identified in all cases. Other proteins previously detected in NFTs were also abundant including: ubiquitin (Perry *et al.*, 1987), neurofilament light, medium and heavy polypeptides (Vickers *et al.*, 1994), APOE (Namba *et al.*, 1991), GAPDH (Wang *et al.*, 2005) and CDK5 (Augustinack *et al.*, 2002). Amyloid-β was not detected in NFTs.

Enrichment analyses were performed to identify protein families/pathways that were enriched in NFTs. These analyses showed that tau was the most significant

upstream regulator of proteins present in NFTs (104 proteins regulated by tau; $P = 1.17 \times 10^{-94}$; Supplementary Data 1). NFTs were highly enriched in proteins associated with neurological diseases (336 proteins), notably including proteins associated with movement disorders ($P = 1.17 \times 10^{-60}$), tauopathy ($P = 5.61 \times 10^{-33}$) and Alzheimer's disease ($P = 3.89 \times 10^{-29}$). Pathway analysis showed that proteins involved in mitochondrial dysfunction ($P = 2.10 \times 10^{-18}$), EIF2 signalling ($P = 3.84 \times 10^{-18}$), phagosome maturation ($P = 2.68 \times 10^{-15}$) and 14-3-3 signalling ($P = 5.23 \times 10^{-15}$) were particularly enriched. It was also of note that proteins involved in the protein ubiquitination pathway (2.97×10^{-11}) and the unfolded protein response ($P = 8.37 \times 10^{-9}$) were also enriched. Specific protein families were also particularly enriched in NFTs including RNA binding proteins and heat-shock protein 70 and 90 families (Fig. 1).

Phosphorylated tau interactome in sporadic Alzheimer's disease

Our NFT proteome results provide the most comprehensive profile of proteins present in NFTs to date. However, one limitation of this approach is that it cannot be determined from this dataset whether the proteins identified in NFTs were present because they directly interacted with pTau or if they were neuronal proteins that were present by chance in NFTs. Therefore, we performed a second, complementary proteomic analysis to identify proteins that directly interacted with pTau, which together form the pTau interactome. To this end, we performed AP-MS using the anti-pTau antibody PHF1 to co-immunoprecipitate pTau and its binding partners. PHF1 was selected because it is a widely used antibody that recognizes pTau species that are abundant in NFTs and dystrophic neurites in Alzheimer's disease. Co-IP was performed on frontal cortex tissue from five cases of advanced sporadic Alzheimer's disease. Two co-IPs were performed on each case, the first using PHF1 and the second using an isotype control IgG antibody, resulting in 10 samples that were individually analysed using LC-MS. Across the 10 samples, 1194 proteins were detected (after removal of all IgG identifications and any duplicate proteins; Supplementary material).

Characterization of the co-immunoprecipitated phosphorylated tau species

As expected, tau was the most abundant protein detected in the PHF1 co-IP samples. One hundred and sixty-six unique tau peptides were identified in this study (taking into account the presence of post-translational modifications). Analysis of tau specific peptides showed evidence of all six human tau isoforms (Supplementary material). Twenty-three different phosphorylated residues on tau were identified on the co-immunoprecipitated tau species (Fig. 2 and Supplementary material), importantly including phosphorylation of serine 396 and serine 404, which are the phosphorylated residues that the PHF1 antibody recognizes. The most abundant tau peptide detected in this study was one containing the S396 phosphorylated residue. This peptide was detected in all five PHF1 co-IP samples and not in any IgG control co-IP samples, providing evidence that the PHF1 co-IP abundantly and specifically isolated the disease-associated pTau species that we were targeting from Alzheimer's disease brains. We were surprised to identify so many phosphorylated residues on tau given that we did not enrich for phosphopeptides prior to LC-MS (as has been necessary in prior studies, Dammer *et al.*, 2015) and because tau is known to undergo rapid dephosphorylation with increased post-mortem interval in mice (Wang *et al.*, 2015). Our robust identification of phosphorylated tau peptides suggest that these species of phosphorylated tau are still detectable even after an extended post-mortem interval, possibly because of their presence in NFTs.

The phosphorylated tau interactome

We identified pTau interactors using the SAINT algorithm, which determines the statistical probability that a given protein is a *bona fide* interactor. A SAINT score for each protein was determined: 1 = highest probability of being a *bona fide* interactor; and 0 = lowest probability of being a *bona fide* interactor. For our analysis any protein with a SAINT score $\geqslant 0.65$ was considered to be a pTau interactor. At this stringency, 125 proteins were identified as pTau interactors, including many proteins known to interact with pTau such as ubiquitin, apolipoprotein E and sequestosome-1 (Fig. 3 and Supplementary material). Amyloid-β was not identified as a pTau interactor. Multiple protein families were significantly enriched in the pTau interactome including 14-3-3 family, microtubule binding proteins and protein families related to the proteasome (Fig. 3).

Network analysis showed that the pTau interactome was most significantly enriched in proteins involved in the ubiquitin-proteasome system (Fig. 3; 17 proteins; $P = 2.49 \times 10^{-13}$). It is well established that pTau is ubiquitinated, and therefore it was not surprising to find an interaction between pTau and multiple forms of ubiquitin (UBB/UBC and UBA52). In addition, we observed a significant interaction between pTau and 10 of 20 protein subunits of the 19S regulatory lid of the proteasome including PSMC1, PSMC2, PSMC3, PSMC4, PSMC5, PSMD2, PSMD3, PSMD8, PSMD11, and PSMD13. In contrast, we did not observe an interaction between pTau and any 20S protein subunit. Combined, these results provide evidence that PHF1 immunoreactive pTau is ubiquitinated and directly binds to the 19S lid of the proteasome.

The pTau interactome was also enriched in proteins involved in phagosome maturation (Fig. 3; 10 proteins; $P = 1.26 \times 10^{-8}$), including three subunits of the vacuolar ATPase that acidifies vesicles (ATP6V0D1, ATP6V1B2, ATP6V1H) and three members of the SNARE complex that

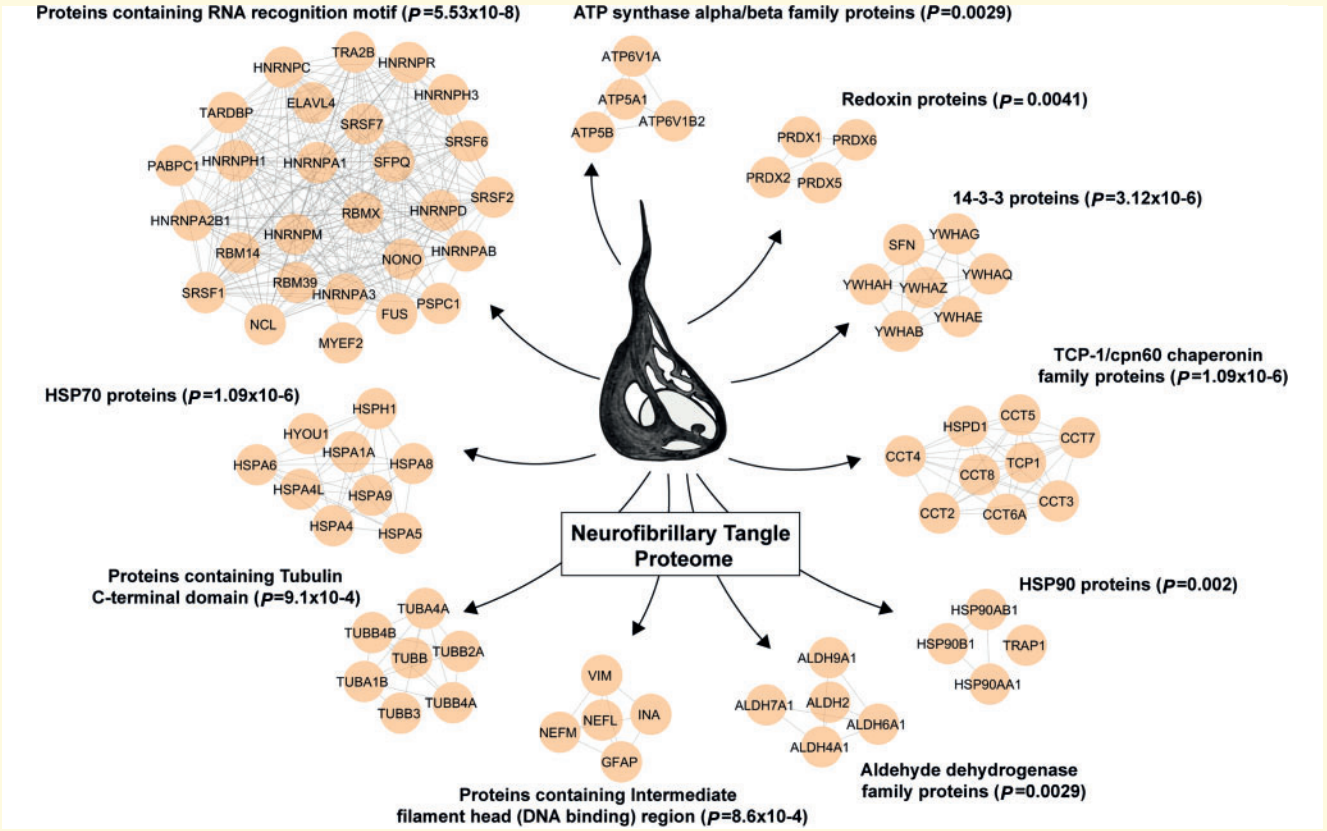

Figure 1 Protein families that were most enriched in NFTs in advanced Alzheimer's disease. Enrichment of protein families was determined using PFAM enrichment analysis within STRING. The protein families that were most significantly enriched in NFTs are shown.

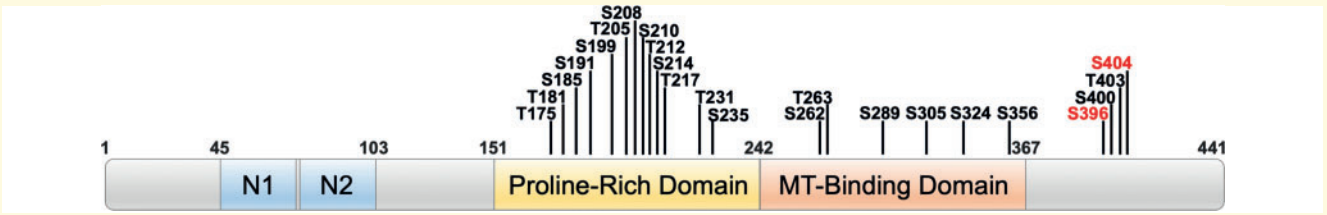

Figure 2 Phosphorylated residues identified to be present on tau by AP-MS. Numbering corresponds to the longest tau isoform (441 amino acids in length). Phosphorylated residues recognized by PHF1 are shown in red.

mediates vesicle fusion to membranes (VAMP2, NSF, NAPB). We also found a significant enrichment in proteins associated with necrosis (56 proteins; $P = 2.26 \times 10^{-11}$). A conspicuous lack of interaction between pTau and tubulins was evident; TUBA8 was the only tubulin identified as a significant pTau binding protein. This finding is consistent with the fact that tau detaches from microtubules after phosphorylation. Interestingly, there was still a significant interaction observed between pTau and other microtubule associated proteins including MAP1B, MAP2 and MAP4, suggesting that this interaction remains after phosphorylation.

Comparison of our pTau interactome with the human kinome (Manning *et al.*, 2002) identified four kinases that significantly interacted with pTau; CAMK2A, CAMK2B, CAMK2D and CDK5. This suggests that these kinases may be particularly involved in phosphorylation of PHF1-immunoreactive pTau. An additional 17 kinases were identified in our AP-MS study; however, the probability of these kinases having a *bona fide* interaction with pTau did not reach our required level of statistical significance. Comparison of the pTau interactome with a comprehensive list of all human phosphatases (Sacco *et al.*, 2012) revealed that PPP2R1A was the only phosphatase that was found to significantly interact with pTau. PPP2R1A is a regulatory subunit of protein phosphatase 2A, which is known to dephosphorylate tau (Sontag *et al.*, 1996) and was recently identified as a

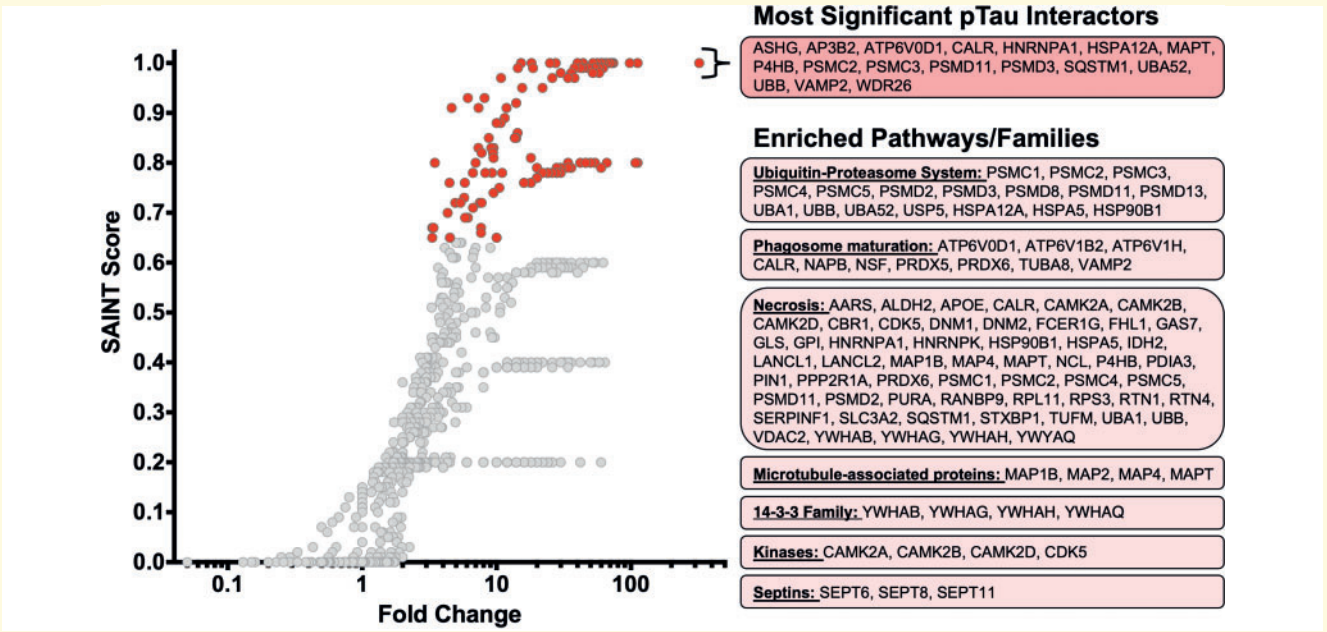

Figure 3 Proteins identified by AP-MS for pTau. Each point corresponds to an individual protein plotted by fold change difference after co-IP for pTau versus isotype control antibody (*x*-axis) and the probability that a protein is a pTau interactor (SAINT score; *y*-axis). SAINT score = 1 identifies proteins with the highest probability of being a pTau interactor (proteins with a SAINT score = 1 detailed in the box labelled 'most significant pTau interactors'). One hundred and twenty-five proteins were found to be significant pTau interactors (highlighted in red). Enriched pathways/families highlights examples of the most significantly enriched protein pathways or families identified by enrichment analysis.

new genetic variant associated with sporadic Alzheimer's disease (Miron *et al.*, 2019). Our results also therefore confirm the involvement of PP2A as the primary phosphatase that interacts with PHF1 immunoreactive pTau.

A cell-type-specific analysis of the pTau interactome showed that pTau interacting proteins were significantly more likely to be neuron specific proteins ($P = 2.74 \times 10^{-5}$). In contrast, there was no enrichment of astrocyte, microglia, oligodendroglia or endothelial specific proteins in the pTau interactome. Neuron-specific proteins in the pTau interactome included HSPA12A, SNAP91, OXCT1, STXBP1, YWHAG, DNM1, NSF, CKMT1A, NAPB, MAP2, YWHAH, AP3B2, RTN1, SYNGR3, MAP1B and TUBA8. Astrocyte specific proteins included APOE and IDH2. FCER1G, PIP4K2A and KIF5A were the only microglia, oligodendrocyte and endothelial specific proteins identified in the pTau interactome respectively. These results confirm the PHF1 immunoreactive pTau predominantly interacts with proteins inside neurons rather than interacting with proteins present in other cell types.

Comparison of proteins found in neurofibrillary tangles and the phosphorylated tau interactome

The overall goal of our study was to identify the proteins present in NFTs that directly interacted with pTau, as these are most likely be of pathological importance in Alzheimer's disease. Therefore, we compared our NFT proteome with the pTau interactome. As expected, there was significant overlap between the two studies; 75 of the 125 pTau interactome proteins were present in NFTs (Tables 2, 3, Fig. 4 and Supplementary material).

This subset of 75 proteins was most significantly enriched in proteins involved in phagosome maturation (enrichment $P = 3.96 \times 10^{-8}$; 8/75 proteins; ATP6V0D1, ATP6V1B2, ATP6V1H, NAPB, NSF, PRDX5, PRDX6, VAMP2). Four of 75 proteins were 14-3-3 protein family members (including 14-3-3 gamma, theta, eta and beta/alpha). This subset was also enriched in DNA binding proteins (six proteins; enrichment $P = 0.00027$; HNRNPK, HNRNPA2B1, HNRNPA1, SSBP1, MAPT, PURA) and proteins that regulate synaptic plasticity (10 proteins; 2.88×10^{-6}).

Fifty pTau interacting proteins were not found in NFTs (Supplementary material). A closer analysis of these 50 proteins showed that 25 were actually detected in NFTs in our study, but were only present in two or fewer cases, and were therefore removed from further analysis in the NFT data set based on our stringency criteria (Supplementary material). These proteins typically were detected with low abundance in NFTs. The remaining 25 proteins were not detected in NFTs in any case and may represent a unique subset of proteins that interact with pTau outside of NFTs.

Comparison of the phosphorylated tau interactome with previously published studies

To place our results in the context of what is already known about proteins that are associated with tau, we compared our pTau interactome with previously published studies using a combination of systematic literature searches and data mining of previous proteomics studies. We found that 98% of the 125 proteins in our pTau interactome had been previously associated with Alzheimer's disease (122 proteins; Supplementary material). These previous findings confirm that the pTau interactome proteins that we identified are already known to be proteins of interest for Alzheimer's disease. We were then interested to determine which pTau interactome proteins had been previously associated with tau. Tau association was designated if there was published evidence of co-localization in NFTs, interaction with tau, or if a protein was mechanistically linked to tau in a targeted study. Ninety-six (77%) of the pTau interactome proteins were associated with tau in previous studies; 33 that were directly associated with pTau and 63 that were associated with tau generally, therefore, validating our results (Supplementary material). The high degree of overlap between our results and previous studies provides additional confidence in the 29 novel pTau interacting proteins that we identified. Importantly, 26 of these novel proteins have been previously associated with Alzheimer's disease, therefore, here we provide new evidence that the involvement of these proteins in Alzheimer's disease likely involves interaction with tau.

Validation of AP-MS results

HPS90B1 was selected as an example protein for validation studies based on its presence in NFTs, the high number of peptides identified after AP-MS (suggestive of a significant interaction with pTau), the availability of an appropriate commercial antibody and no previous evidence of interaction with pTau in human Alzheimer's disease brain tissue. We confirmed that immunoprecipitation for HPS90B1 resulted in the abundant co-IP of pTau (Fig. 5), therefore providing additional validation of our AP-MS results. Co-IPs for two additional proteins were also included in this validation study, one that acted as a positive control (secernin-1, SCRN1) and one that acted as a negative control (ezrin, EZR). We recently identified SCRN1 as a novel pTau interacting protein that co-localizes with pTau aggregates in Alzheimer's disease, but not in other tauopathies (Pires *et al.*, 2019). In the current study, we confirmed that SCRN1 had a significant interaction with pTau (SAINT score = 0.92) and validation studies confirmed that immunoprecipitation of SCRN1 resulted in the co-IP of pTau (Fig. 5). EZR was included as an example negative control protein based on its significant increase in Alzheimer's disease brain tissue (Hondius *et al.*, 2016; Seyfried *et al.*, 2017; Johnson *et al.*, 2018; Zhang *et al.*, 2018; Xu *et al.*, 2019) and abundant presence in amyloid plaques (Drummond *et al.*, 2017), but no evidence of direct interaction with pTau in our study. Accordingly, immunoprecipitation of EZR did not result in the co-IP of pTau, therefore providing a negative control for our validation studies provides support for the specificity of the interaction between HSP90B1 and pTau (Fig. 5).

Discussion

We have generated a comprehensive profile of the pTau interactome in the human Alzheimer's disease brain. Our two complementary proteomics approaches allowed us to determine the proteins present in NFTs and the proteins that interact with pTau. Combined analysis of data generated using both of these approaches identified 75 proteins that are both present in NFTs and significantly interact with pTau. These results are the first to comprehensively define the proteins that interact with disease-associated pTau species in Alzheimer's disease; all previous similar studies have identified proteins that interact with any species of tau, including physiological, non-phosphorylated tau (Meier *et al.*, 2015; Ayyadevara *et al.*, 2016; Liu *et al.*, 2016; Wang *et al.*, 2017; Maziuk *et al.*, 2018; Hsieh *et al.*, 2019). Despite these differences we were pleased to see a significant overlap between our results and previous total tau interactome studies; 84% of proteins that were present in NFTs and interacted with pTau in our study, have been associated with tau in previous studies, therefore validating our results. Importantly our study confirms that these proteins specifically interact with pTau in human Alzheimer's disease brain tissue, suggesting that they are excellent candidates for future studies examining the toxic role of tau in Alzheimer's disease. Excitingly, we identified an additional 12 proteins that were both present in NFTs and interacted with pTau that have not yet been associated with tau. Therefore, we provide new evidence about their association with tau and increased understanding about how they may be involved in Alzheimer's disease.

The pTau interactome was significantly enriched in neuron-specific proteins. Very little interaction between pTau and proteins specific to astrocytes, microglia, oligodendrocytes or epithelial cells was observed. This is to be expected given the intraneuronal location of pTau and NFTs in Alzheimer's disease. Enrichment analyses showed that the pTau interactome was most significantly enriched in proteins associated with the two main protein degradation systems in the cell; the ubiquitin-proteasome system and the phagosome-lysosome system. The ubiquitin-proteasome system recycles damaged or misfolded proteins. Proteins are tagged with ubiquitin, which signals them to be trafficked to the proteasome with the assistance of chaperone proteins for degradation. Our AP-MS studies showed that pTau directly interacted with proteins involved in all aspects of this system including enzymes responsible for ubiquitination of proteins, ubiquitin itself,

Table 2 pTau interacting proteins present in NFTs (novel pTau interactors)

Protein name (gene)	Fold change	SAINT Score	Known Interaction - Total Tau
Published association with tau, but not with pTau or NFTs			
Vesicle-associated membrane protein 2 (*VAMP2*)	40	1	Interacts in human brain[a]
Heat shock 70 kDa protein 12A (*HSPA12A*)	74	1	Interacts in human[a,b] and mouse brain[c]
V-type proton ATPase subunit d 1 (*ATP6V0D1*)	44	1	Interacts in human brain[d]
26S protease regulatory subunit 7 (*PSMC2*)	66	1	Functional[g]; Interacts in human brain[a]
Elongation factor Tu, mitochondrial (*TUFM*)	58	0.99	Interacts in mouse brain[c]
Clathrin coat assembly protein AP180 (*SNAP91*)	44	0.99	Interacts in mouse brain[c]
Transcriptional activator protein Pur-alpha (*PURA*)	48	0.99	Interacts in mouse brain[c]
LanC-like protein 1 (*LANCL1*)	14.4	0.99	Interacts in human[a,d] and mouse brain[c]
Isocitrate dehydrogenase [NADP], mitochondrial (*IDH2*)	54	0.99	Interacts in human brain[a]
Actin-related protein 2/3 complex subunit 4 (*ARPC4*)	30	0.98	Interacts in mouse brain[c]
Eukaryotic initiation factor 4A-II (*EIF4A2*)	38	0.97	Interacts in human[a] and mouse brain[f]
Ubiquitin carboxyl-terminal hydrolase 5 (*USP5*)	15.5	0.95	Interacts in human[a] and mouse brain[c]
Phosphoglycerate mutase (*PGAM1*)	6.12	0.93	Interacts in human[a,b] and mouse brain[e,f]
Endoplasmin (Grp94) (*HSP90B1*)	7.35	0.91	Interacts in mouse brain[c]
Vesicle-fusing ATPase (*NSF*)	10.71	0.88	Interacts in human[a] and mouse brain[c,e]
Creatine kinase U-type, mitochondrial (*CKMT1A*)	7.75	0.82	Interacts in mouse brain[e]
WD repeat-containing protein 1 (*WDR1*)	9.5	0.81	Interacts in human brain[a]
Beta-soluble NSF attachment protein (*NAPB*)	7	0.8	Interacts in human brain[a,b]
26S proteasome non-ATPase regulatory subunit 2 (*PSMD2*)	66	0.8	Functional[g]; interacts in human brain[a]
Ubiquitin-like modifier-activating enzyme 1 (*UBA1*)	20	0.79	Interacts in human[a,b] and mouse brain[c]
Reticulon-4 (*RTN4*)	28	0.79	Interacts in human brain[a]
Alanine–tRNA ligase, cytoplasmic (*AARS*)	36	0.79	Interacts in human[a] and mouse brain[c]
Band 4.1-like protein 3 (*EPB41L3*)	11	0.78	Interacts in human brain[a,b,d]
Peroxiredoxin-5, mitochondrial (*PRDX5*)	24	0.78	Interacts in mouse brain[c,e]
Serine/arginine-rich splicing factor 7 (*SRSF7*)	30	0.78	Functional[h]
Cell cycle exit and neuronal differentiation protein 1 (*CEND1*)	24	0.78	Interacts in mouse brain[e]
60S ribosomal protein L11 (*RPL11*)	20	0.77	Interacts in human brain[a]
Transketolase (*TKT*)	4.47	0.76	Interacts in mouse brain[c]
78 kDa glucose-regulated protein (*HSPA5*)	4.93	0.72	Interacts in mouse brain[c]
Microtubule-associated protein 4 (*MAP4*)	7.75	0.72	Functional[i]
V-type proton ATPase subunit B, brain isoform (*ATP6V1B2*)	6.12	0.69	Interacts in mouse brain[c]
ATP-dependent 6-phosphofructokinase, platelet type (*PFKP*)	7.67	0.66	Interacts in human[a,b] and mouse brain[c]
Pyruvate dehydrogenase E1 component subunit beta, mitochondrial (*PDHB*)	4.5	0.65	Interacts in mouse brain[c]
Cytosolic non-specific dipeptidase (*CNDP2*)	4.5	0.65	Interacts in human brain[a]
Novel tau associated proteins			
Heterogeneous nuclear ribonucleoprotein A1 (*HNRNPA1*)	62	1	Novel
Succinyl-CoA : 3-ketoacid-coenzyme A transferase (*OXCT1*)	62	0.99	Novel
Immunoglobulin superfamily member 8 (*IGSF8*)	52	0.98	Novel
Histone H2A type 1-B/E (*HIST1H2AB*)	13.67	0.85	Novel
Histone H2A type 1-H (*HIST1H2AH*)	14	0.85	Novel
Cytochrome c oxidase subunit 5B, mitochondrial (*COX5B*)	34	0.8	Novel
Elongation factor 1-gamma (*EEF1G*)	42	0.8	Novel
V-type proton ATPase subunit H (*ATP6V1H*)	28	0.79	Novel
Single-stranded DNA-binding protein (*SSBP1*)	24	0.78	Novel
Voltage-dependent anion-selective channel protein 2 (*VDAC2*)	5.4	0.72	Novel
40S ribosomal protein S3 (*RPS3*)	7.67	0.67	Novel
Histone H2B (*HIST1H2BJ*)	10	0.65	Novel

Proteins listed in order of SAINT score. Fold change refers to the fold change difference in interaction with PHF1 versus control IgG. 'Functional' refers to a reported functional association between pTau and protein. Additional information about previously reported interactions available in Supplementary Table 2.
[a]Hsieh *et al.*, 2019; [b]Ayyadevara *et al.*, 2016; [c]Wang *et al.*, 2017; [d]Meier *et al.*, 2015; [e]Liu *et al.*, 2016; [f]Maziuk *et al.*, 2018; [g]Myeku *et al.*, 2016; [h]Gao *et al.*, 2007; [i]Dehmelt and Halpain, 2005.

molecular chaperones involved in transporting ubiquitinated proteins and subunits of the proteasome. It is well known that aggregated tau present in NFTs is highly ubiquitinated (Mori *et al.*, 1987; Perry *et al.*, 1987). It has been hypothesized that the accumulation of ubiquitinated tau in Alzheimer's disease is because either the ubiquitin-proteasome system is impaired in Alzheimer's disease (Keller *et al.*, 2000; Keck *et al.*, 2003) or because the proteasome

Table 3 pTau interacting proteins present in NFTs (previously validated pTau interactors)

Protein name	Fold change	SAINT Score	Known interaction: total tau	Known interaction: pTau
Ubiquitin (*UBB; UBC*)	15.21	1	Functional[a]; interacts in human brain[b,c]	In NFTs[d]
Microtubule-associated protein tau (*MAPT*)	52.22	1	Tau itself	In NFTs[e]
Protein disulfide-isomerase (*P4HB*)	25	1	Functional[f]; interacts in human brain[b]	In NFTs[g]
Sequestosome-1 (*SQSTM1*)	322	1	Functional[h]; interacts in human brain[b,c]	In NFTs[i]
Glucose-6-phosphate isomerase (*GPI*)	18.67	0.99	Interacts in human brain[b]	In NFTs[j]
Glutaminase kidney isoform, mitochondrial (*GLS*)	58	0.98	Interacts in mouse brain[k]	In NFTs[l]
Calcium/calmodulin-dependent protein kinase type II subunit alpha (*CAMK2A*)	10.8	0.97	Interacts in human[b] and mouse brain[k]	Functional[m]; in NFTs[j]
Adenylate kinase isoenzyme 1 (*AK1*)	26	0.97	Interacts in human brain[b]	Functional[n]
Syntaxin-binding protein 1 (*STXBP1*)	8.13	0.93	Interacts in human[b] and mouse brain[k,o]	Functional[p]; in NFTs[q]
Secernin-1 (*SCRN1*)	14	0.92	Interacts in human brain[b]	In NFTs[r]; interacts with pTau[r]
14-3-3 protein gamma (*YWHAG*)	4.63	0.91	Interacts in human[b,c] and mouse brain[k]	Functional[s]; in NFTs[t]
Dynamin-1 (*DNM1*)	11.86	0.91	Interacts in human[b,c] and mouse brain[k,o]	In NFTs[j]
Carbonyl reductase [NADPH] 1 (*CBR1*)	7.33	0.83	Interacts in human brain[b,c]	In NFTs[u]
Heterogeneous nuclear ribonucleoproteins A2/B1 (*HNRNPA2B1*)	9.14	0.83		In NFTs[v]
Calcium/calmodulin-dependent protein kinase type II subunit beta (*CAMK2B*)	9.4	0.82	Interacts in human brain[b]	Functional[w]
Heterogeneous nuclear ribonucleoprotein K (*HNRNPK*)	18	0.81	Functional[x]	In NFTs[j]
Microtubule-associated protein 2 (*MAP2*)	112	0.8	Functional[y]; interacts in human brain[b]	Interacts with pTau[z]
Nucleolin (*NCL*)	46	0.8	Functional[aa]	In NFTs[bb]
Serine/threonine-protein phosphatase 2A 65 kDa regulatory subunit A alpha isoform (*PPP2R1A*)	34	0.79	Interacts in human[b] and mouse brain[a,cc]	Functional[dd]
Apolipoprotein E (*APOE*)	9.25	0.78	Interacts in human[b,c,ee] and mouse brain[o]	Functional[ff]
Peptidyl-prolyl cis-trans isomerase NIMA-interacting 1 (*PIN1*)	28	0.78	Interacts in human brain[b]	Functional[gg]; in NFTs[gg]
Cyclin-dependent-like kinase 5 (*CDK5*)	24	0.78	Interacts in human brain[b]	Functional[hh]
Carbonic anhydrase 2 (*CA2*)	18	0.76		In NFTs[j]
Peroxiredoxin-6 (*PRDX6*)	5.75	0.73		In NFTs[j]
Microtubule-associated protein 1B (*MAP1B*)	6.69	0.71	Functional[y]; interacts in human brain[b,c]	Interacts with pTau[z]
Aldehyde dehydrogenase, mitochondrial (*ALDH2*)	5.83	0.69		Functional[ii]
14-3-3 protein theta (*YWHAQ*)	3.32	0.67	Interacts in human[b] and mouse brain[k]	Functional[s]
14-3-3 protein beta/alpha (*YWHAB*)	3.39	0.67	Interacts in human[b,c,ee] and mouse brain[k]	Functional[s]; in NFTs[ii]; interacts with pTau[kk]
14-3-3 protein eta (*YWHAH*)	3.32	0.65	Interacts in human[b,ee] and mouse brain[k]	Functional[s]; interacts with pTau[kk]

Proteins listed in order of SAINT score. Fold change refers to the fold change difference in interaction with PHF1 versus control IgG. Functional refers to a reported functional association between pTau and protein. Additional information about previously reported interactions available in Supplementary Table 2.

[a]Lee *et al.*, 2013; [b]Hsieh *et al.*, 2019; [c]Ayyadevara *et al.*, 2016; [d]Perry *et al.*, 1987; [e]Grundke-Iqbal *et al.*, 1986; [f]Xu *et al.*, 2013; [g]Honjo *et al.*, 2010; [h]Babu *et al.*, 2005; [i]Kuusisto *et al.*, 2002; [j]Wang *et al.*, 2005; [k]Wang *et al.*, 2017; [l]Kowall and Beal, 1991; [m]Yoshimura *et al.*, 2003; [n]Park *et al.*, 2012; [o]Liu *et al.*, 2016; [p]Shetty *et al.*, 1995; [q]Takahashi *et al.*, 2000; [r]Pires *et al.*, 2019; [s]Chen *et al.*, 2019; [t]Umahara *et al.*, 2004; [u]Minjarez *et al.*, 2013; [v]Mizukami *et al.*, 2005; [w]Ferrer *et al.*, 2001; [x]Liu and Szaro, 2011; [y]Dehmelt and Halpain, 2005; [z]Alonso *et al.*, 1997; [aa]Sjoberg *et al.*, 2006; [bb]Dranovsky *et al.*, 2001; [cc]Maziuk *et al.*, 2018; [dd]Taleski and Sontag, 2018; [ee]Meier *et al.*, 2015; [ff]Shi *et al.*, 2017; [gg]Lu *et al.*, 1999; [hh]Baumann *et al.*, 1993; [ii]Ohsawa *et al.*, 2008; [jj]Sugimori *et al.*, 2007; [kk]Sadik *et al.*, 2009.

is unable to degrade pTau (Poppek *et al.*, 2006). The proteasome is known to have an important role in tau degradation (David *et al.*, 2002). Intriguingly, pTau has been shown to inhibit proteasome function (Keck *et al.*, 2003; Myeku *et al.*, 2016), and this inhibition of the proteasome results in the accelerated formation of tau inclusions (Goldbaum *et al.*, 2003; Tan *et al.*, 2008). Combined with our results, these studies support the hypothesis that pTau may inhibit the proteasome in Alzheimer's disease, which has likely downstream consequences of increased pTau accumulation and an overall decrease in protein degradation.

Our results show interaction between pTau and 10 subunits of the 19S proteasome regulatory lid, but not any subunit of the 20S catalytic core particle where proteolysis occurs. One interpretation of these results is that ubiquitinated pTau is trafficked to the proteasome for degradation where it binds to the 19S regulatory lid of the proteasome, but is unable to enter the catalytic core of the proteasome (likely because of the large size of pTau aggregates). The interaction between pTau and the 19S proteasome regulatory lid could then physically block the proteasome pore and inhibit general proteasome function.

We also showed that pTau interacts with proteins involved in the phagosome-lysosome system. We confirmed the known interaction between tau and sequestosome-1 (also known as p62), which is a major cargo protein that directs bound proteins for both autophagy and degradation by the proteasome (Salminen *et al.*, 2012). Interestingly we also observed an interaction between pTau and 3 of 14 subunits of the vacuolar ATPase (v-ATPase) proton pump, which is responsible for acidifying lysosomes. Impairment of v-ATPases have been associated with the pathogenesis of Alzheimer's disease (Colacurcio and Nixon, 2016), but no study has yet linked v-ATPase impairment with pTau. Pathological species of tau have been shown to cause morphological abnormalities and dysfunction of lysosomes *in vitro* (Wang *et al.*, 2009) and in transgenic mice (Lim *et al.*, 2001; Collin *et al.*, 2014; Feng *et al.*, 2020). Impaired lysosome morphology is also present in human brain tissue from patients with tau-only dementias such as corticobasal degeneration and progressive supranuclear palsy (Piras *et al.*, 2016). More study is needed to analyse the interaction between v-ATPases and tau, but our results suggest that it is possible that pTau could contribute to lysosomal dysfunction in Alzheimer's disease via interaction with v-ATPases. Impairment of both main protein degradation systems would result in accumulation of many different waste proteins in the cell. Interestingly, tau has recently been shown to undergo liquid phase transition, which causes localized molecular crowding, enhances the opportunity for interaction with other proteins, and can promote the formation of oligomers (Wegmann, 2019). We observed that tau interacted with a number of other proteins that also undergo liquid phase transition (HNRNPA1, SQSTM1, HNRNPA2B1 and UBB) (Li *et al.*, 2020), suggesting that these interactions may possibly facilitate such phase transitions for other proteins.

One important limitation of this study is that our pTau interactome is restricted to those proteins that interact with

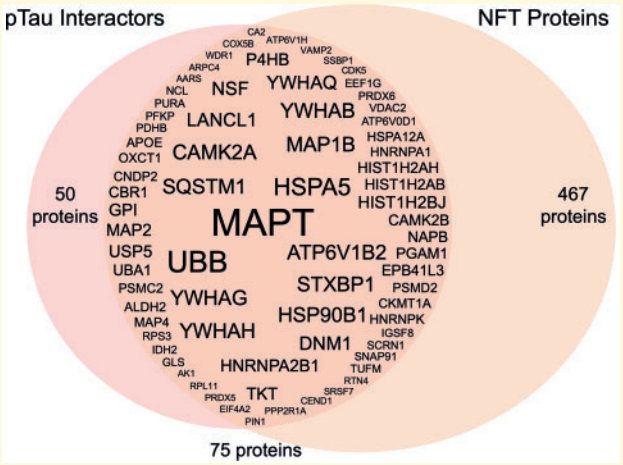

Figure 4 Overlap of pTau interactors and proteins found in NFTs. Seventy-five proteins present in NFTs were also significant pTau interactors. Overlapping proteins are shown by gene IDs, with the font size corresponding to the number of peptide spectrum matches for each protein after pTau AP-MS. As expected, tau (MAPT) was the most abundant protein identified after AP-MS, followed by ubiquitin (UBB).

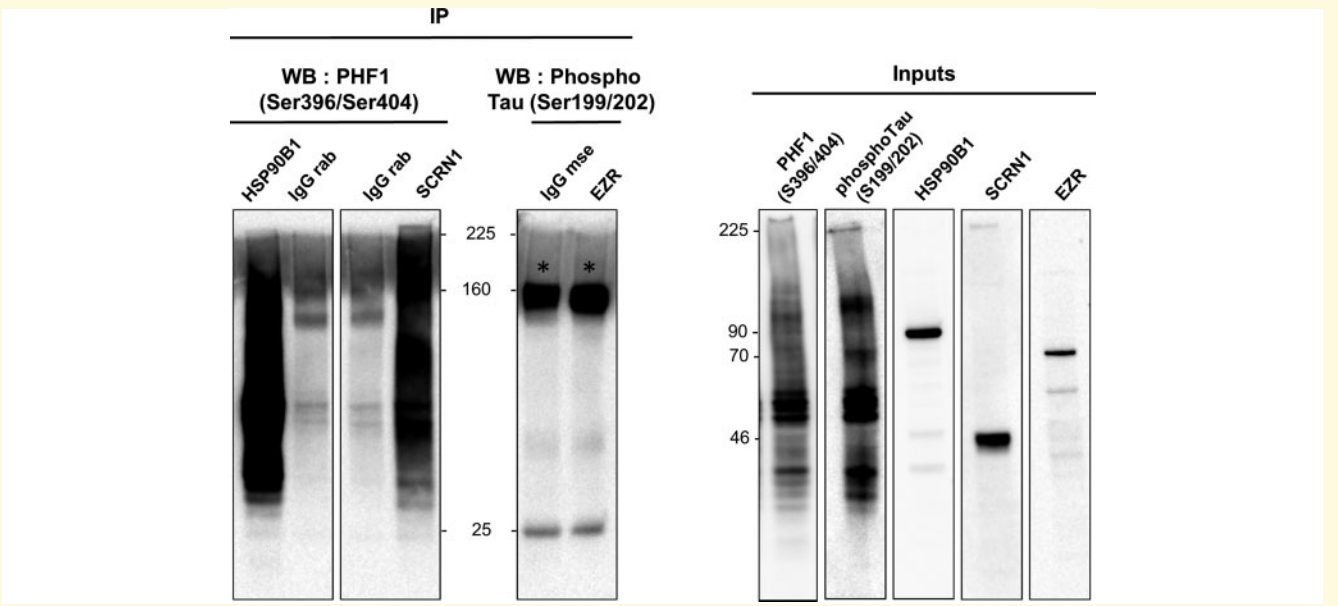

Figure 5 Validation of AP-MS results using co-IP. Validation of HSP90B1, SCRN1 (positive control) and EZR (negative control) interactions with pTau. Co-IP was performed on fresh frozen frontal cortex tissue from one Alzheimer's disease case. Immunoprecipitation was performed using anti-HSP90B1, anti-SCRN1, anti-EZR, rabbit IgG isotype control or mouse IgG isotype control. Both HSP90B1 and SCRN1 pulled down pTau, while EZR did not. Presence of pTau, HPS90B1, SCRN1 and EZR in input brain homogenate was confirmed. Asterisks indicate bands corresponding to cross-reactive IgGs.

species of tau that are immunoreactive to PHF1. PHF1 recognizes tau phosphorylated at serines 396 and 404, which is typically found in mature NFTs (Greenberg *et al.*, 1992; Otvos *et al.*, 1994) and therefore, our interactome results do not provide insight into proteins that uniquely interact with unphosphorylated tau or tau species that are phosphorylated at other residues but not at S396 or S404. In the future, studies that use a similar approach using antibodies that recognize other forms of pTau, especially those forms that are present in early Alzheimer's disease, would be useful to provide a more complete picture of pTau interactions throughout the progression of Alzheimer's disease. In addition, it is important to note that the pTau interacting proteins reported in this study are limited to those that interact with PHF1 immunoreactive tau specifically in Alzheimer's disease and not necessarily PHF1 immunoreactive species in other tauopathies. Recent studies have shown that pTau aggregates have significantly different conformations in Alzheimer's disease and Pick's disease (Fitzpatrick *et al.*, 2017; Falcon *et al.*, 2018*a*, *b*) and this different conformation would likely result in different protein interactions. Our recent findings showing that secernin-1 specifically interacts with PHF1 immunoreactive pTau in Alzheimer's disease but not in other tauopathies supports this hypothesis (Pires *et al.*, 2019). In addition, it is also important to note that the pTau interactors that we have identified may not exclusively interact with pTau. While this may be the case for some proteins, it is also likely that some proteins interact with both non-phosphorylated tau and pTau. Future studies directly comparing the interaction of these proteins with non-phosphorylated tau and pTau will clarify which of these proteins exclusively interact with pTau. Another important consideration is that pTau interactors identified in this study may not necessarily directly bind to pTau; their interaction with pTau may result from an interaction between pTau and members of a protein complex that these proteins belong to. Future mechanistic studies will help determine which of these proteins directly interact with pTau and which are indirectly interacting with pTau as part of a protein complex. Therefore, our results provide the first piece of a complex puzzle of tau pathophysiology in Alzheimer's disease. Despite these limitations we were pleased to see that we identified many of the proteins previously associated with pTau in targeted studies as well as many proteins that have already been implicated in Alzheimer's disease pathogenesis. This strongly suggests that our approach identified tau interacting proteins that are pathologically relevant in Alzheimer's disease.

In conclusion, we present a comprehensive analysis of the pTau interactome in the human Alzheimer's disease brain. Unbiased proteomics studies, such as this one, are an essential step to enhance our understanding about Alzheimer's disease pathogenesis (Drummond and Wisniewski, 2017, 2019; Drummond *et al.*, 2018*a*). It is our hope that this resource will help uncover new biomarkers of disease, novel drug targets and will increase our understanding about the pathological role of tau in Alzheimer's disease.

Funding

This work was supported by funding from the Bluesand Foundation and Dementia Australia to E.D., Philippe Chatrier Foundation to G.P., and National Institutes of Health grants P30AG066512, P01AG060882 and RF1AG058267 to T.W. The proteomics work was in part supported by the NYU School of Medicine and a shared instrumentation grant from the NIH, 1S10OD010582-01A1 for the purchase of an Orbitrap Fusion Lumos.

Competing interests

The authors report no competing interests.

Supplementary material

Supplementary material is available at *Brain* online.

References

Andreev VP, Petyuk VA, Brewer HM, Karpievitch YV, Xie F, Clarke J, et al. Label-free quantitative LC-MS proteomics of Alzheimer's disease and normally aged human brains. J Proteome Res 2012; 11: 3053–67.

Augustinack JC, Sanders JL, Tsai LH, Hyman BT. Colocalization and fluorescence resonance energy transfer between cdk5 and AT8 suggests a close association in pre-neurofibrillary tangles and neurofibrillary tangles. J Neuropathol Exp Neurol 2002; 61: 557–64.

Ayyadevara S, Balasubramaniam M, Parcon PA, Barger SW, Griffin WS, Alla R, et al. Proteins that mediate protein aggregation and cytotoxicity distinguish Alzheimer's hippocampus from normal controls. Aging Cell 2016; 15: 924–39.

Babu JR, Geetha T, Wooten MW. Sequestosome 1/p62 shuttles polyubiquitinated tau for proteasomal degradation. J Neurochem 2005; 94: 192–203.

Baumann K, Mandelkow EM, Biernat J, Piwnica-Worms H, Mandelkow E. Abnormal Alzheimer-like phosphorylation of tau-protein by cyclin-dependent kinases cdk2 and cdk5. FEBS Lett 1993; 336: 417–24.

Bern M, Kil YJ, Becker C. Byonic: advanced peptide and protein identification software. Curr Protoc Bioinformatics 2012; Chapter 13: Unit13.20.

Choi H, Larsen B, Lin ZY, Breitkreutz A, Mellacheruvu D, Fermin D, et al. SAINT: probabilistic scoring of affinity purification-mass spectrometry data. Nat Methods 2011; 8: 70–3.

Colacurcio DJ, Nixon RA. Disorders of lysosomal acidification-the emerging role of v-ATPase in aging and neurodegenerative disease. Ageing Res Rev 2016; 32: 75–88.

Collin L, Bohrmann B, Gopfert U, Oroszlan-Szovik K, Ozmen L, Gruninger F. Neuronal uptake of tau/pS422 antibody and reduced progression of tau pathology in a mouse model of Alzheimer's disease. Brain 2014; 137: 2834–46.

Cox J, Hein MY, Luber CA, Paron I, Nagaraj N, Mann M. Accurate proteome-wide label-free quantification by delayed normalization and maximal peptide ratio extraction, termed MaxLFQ. Mol Cell Proteomics 2014; 13: 2513–26.

Cox J, Neuhauser N, Michalski A, Scheltema RA, Olsen JV, Mann M. Andromeda: a peptide search engine integrated into the MaxQuant environment. J Proteome Res 2011; 10: 1794–805.

Dammer EB, Lee AK, Duong DM, Gearing M, Lah JJ, Levey AI, et al. Quantitative phosphoproteomics of Alzheimer's disease reveals cross-talk between kinases and small heat shock proteins. Proteomics 2015; 15: 508–19.

David DC, Layfield R, Serpell L, Narain Y, Goedert M, Spillantini MG. Proteasomal degradation of tau protein. J Neurochem 2002; 83: 176–85.

Dehmelt L, Halpain S. The MAP2/Tau family of microtubule-associated proteins. Genome Biology 2005; 6: 204.

Drummond E, Goni F, Liu S, Prelli F, Scholtzova H, Wisniewski T. Potential novel approaches to understand the pathogenesis and treat Alzheimer's disease. J Alzheimers Dis 2018a; 64: S299–S312.

Drummond E, Nayak S, Faustin A, Pires G, Hickman RA, Askenazi M, et al. Proteomic differences in amyloid plaques in rapidly progressive and sporadic Alzheimer's disease. Acta Neuropathol 2017; 133: 933–54.

Drummond E, Nayak S, Pires G, Ueberheide B, Wisniewski T. Isolation of amyloid plaques and neurofibrillary tangles from archived Alzheimer's disease tissue using laser-capture microdissection for downstream proteomics. Methods Mol Biol 2018b; 1723: 319–34.

Drummond E, Wisniewski T. Alzheimer's disease: experimental models and reality. Acta Neuropathol 2017; 133: 155–75.

Drummond E, Wisniewski T. Using proteomics to understand Alzheimer's disease pathogenesis. In: Wisniewski T, editor. Alzheimer's disease. Brisbane (AU): Codon Publications; 2019; pp. 37–51.

Drummond ES, Nayak S, Ueberheide B, Wisniewski T. Proteomic analysis of neurons microdissected from formalin-fixed, paraffin-embedded Alzheimer's disease brain tissue. Sci Rep 2015; 5: 15456.

Falcon B, Zhang W, Murzin AG, Murshudov G, Garringer HJ, Vidal R, et al. Structures of filaments from Pick's disease reveal a novel tau protein fold. Nature 2018a; 561: 137–40.

Falcon B, Zhang W, Schweighauser M, Murzin AG, Vidal R, Garringer HJ, et al. Tau filaments from multiple cases of sporadic and inherited Alzheimer's disease adopt a common fold. Acta Neuropathol 2018b; 136: 699–708.

Feng Q, Luo Y, Zhang XN, Yang XF, Hong XY, Sun DS, et al. MAPT/Tau accumulation represses autophagy flux by disrupting IST1-regulated ESCRT-III complex formation: a vicious cycle in Alzheimer neurodegeneration. Autophagy 2020; 16: 641–58.

Fitzpatrick AWP, Falcon B, He S, Murzin AG, Murshudov G, Garringer HJ, et al. Cryo-EM structures of tau filaments from Alzheimer's disease. Nature 2017; 547: 185–90.

Gao L, Wang J, Wang Y, Andreadis A. SR protein 9G8 modulates splicing of tau exon 10 via its proximal downstream intron, a clustering region for frontotemporal dementia mutations. Mol Cell Neurosci 2007; 34: 48–58.

Goldbaum O, Oppermann M, Handschuh M, Dabir D, Zhang B, Forman MS, et al. Proteasome inhibition stabilizes tau inclusions in oligodendroglial cells that occur after treatment with okadaic acid. J Neurosci 2003; 23: 8872–80.

Greenberg SG, Davies P, Schein JD, Binder LI. Hydrofluoric acid-treated tau PHF proteins display the same biochemical properties as normal tau. J Biol Chem 1992; 267: 564–9.

Grundke-Iqbal I, Iqbal K, Quinlan M, Tung YC, Zaidi MS, Wisniewski HM. Microtubule-associated protein tau. A component of Alzheimer paired helical filaments. J Biol Chem 1986; 261: 6084–89.

Hondius DC, van Nierop P, Li KW, Hoozemans JJ, van der Schors RC, van Haastert ES, et al. Profiling the human hippocampal proteome at all pathologic stages of Alzheimer's disease. Alzheimers Dement 2016; 12: 654–68.

Honjo Y, Ito H, Horibe T, Takahashi R, Kawakami K. Protein disulfide isomerase-immunopositive inclusions in patients with Alzheimer disease. Brain Research 2010; 1349: 90–6.

Hsieh YC, Guo C, Yalamanchili HK, Abreha M, Al-Ouran R, Li Y, et al. Tau-mediated disruption of the spliceosome triggers cryptic RNA splicing and neurodegeneration in Alzheimer's disease. Cell Rep 2019; 29: 301–16.e10.

Ittner LM, Ke YD, Delerue F, Bi M, Gladbach A, van Eersel J, et al. Dendritic function of tau mediates amyloid-beta toxicity in Alzheimer's disease mouse models. Cell 2010; 142: 387–97.

Johnson ECB, Dammer EB, Duong DM, Yin L, Thambisetty M, Troncoso JC, et al. Deep proteomic network analysis of Alzheimer's disease brain reveals alterations in RNA binding proteins and RNA splicing associated with disease. Mol Neurodegeneration 2018; 13: 52.

Keck S, Nitsch R, Grune T, Ullrich O. Proteasome inhibition by paired helical filament-tau in brains of patients with Alzheimer's disease. J Neurochem 2003; 85: 115–22.

Keller JN, Hanni KB, Markesbery WR. Impaired proteasome function in Alzheimer's disease. J Neurochem 2000; 75: 436–9.

Kellogg EH, Hejab NMA, Poepsel S, Downing KH, DiMaio F, Nogales E. Near-atomic model of microtubule-tau interactions. Science 2018; 360: 1242–6.

Kowall NW, Beal MF. Glutamate-, glutaminase-, and taurine-immunoreactive neurons develop neurofibrillary tangles in Alzheimer's disease. Ann Neurol 1991; 29: 162–7.

Kramer A, Green J, Pollard J Jr, Tugendreich S. Causal analysis approaches in Ingenuity Pathway Analysis. Bioinformatics 2014; 30: 523–30.

Kuusisto E, Salminen A, Alafuzoff I. Early accumulation of p62 in neurofibrillary tangles in Alzheimer's disease: possible role in tangle formation. Neuropath Appl Neuro 2002; 28: 228–37.

Lee MJ, Lee JH, Rubinsztein DC. Tau degradation: the ubiquitin-proteasome system versus the autophagy-lysosome system. Prog Neurobiol 2013; 105: 49–59.

Li Q, Peng X, Li Y, Tang W, Zhu J, Huang J, et al. LLPSDB: a database of proteins undergoing liquid-liquid phase separation in vitro. Nucleic Acids Res 2020; 48: D320–7.

Lim F, Hernandez F, Lucas JJ, Gomez-Ramos P, Moran MA, Avila J. FTDP-17 mutations in tau transgenic mice provoke lysosomal abnormalities and Tau filaments in forebrain. Mol Cell Neurosci 2001; 18: 702–14.

Litersky JM, Johnson GV, Jakes R, Goedert M, Lee M, Seubert P. Tau protein is phosphorylated by cyclic AMP-dependent protein kinase and calcium/calmodulin-dependent protein kinase II within its microtubule-binding domains at Ser-262 and Ser-356. Biochem J 1996; 316 (Pt 2): 655–60.

Liu C, Song X, Nisbet R, Gotz J. Co-immunoprecipitation with tau isoform-specific antibodies reveals distinct protein interactions and highlights a putative role for 2N tau in disease. J Biol Chem 2016; 291: 8173–88.

Lovestone S, Hartley CL, Pearce J, Anderton BH. Phosphorylation of tau by glycogen synthase kinase-3 beta in intact mammalian cells: the effects on the organization and stability of microtubules. Neuroscience 1996; 73: 1145–57.

Mandelkow EM, Mandelkow E. Biochemistry and cell biology of tau protein in neurofibrillary degeneration. Cold Spring Harb Perspect Med 2012; 2: a006247.

Manning G, Whyte DB, Martinez R, Hunter T, Sudarsanam S. The protein kinase complement of the human genome. Science 2002; 298: 1912–34.

Maziuk BF, Apicco DJ, Cruz AL, Jiang L, Ash PEA, da Rocha EL, et al. RNA binding proteins co-localize with small tau inclusions in tauopathy. Acta Neuropathol Commun 2018; 6: 71.

McInnes J, Wierda K, Snellinx A, Bounti L, Wang YC, Stancu IC, et al. Synaptogyrin-3 mediates presynaptic dysfunction induced by tau. Neuron 2018; 97: 823–35.e8.

Meier S, Bell M, Lyons DN, Ingram A, Chen J, Gensel JC, et al. Identification of novel tau interactions with endoplasmic reticulum proteins in Alzheimer's disease brain. J Alzheimers Dis 2015; 48: 687–702.

Mendonca CF, Kuras M, Nogueira FCS, Pla I, Hortobagyi T, Csiba L, et al. Proteomic signatures of brain regions affected by tau

pathology in early and late stages of Alzheimer's disease. Neurobiol Dis 2019; 130: 104509.
Minjarez B, Valero Rustarazo ML, Sanchez del Pino MM, Gonzalez-Robles A, Sosa-Melgarejo JA, Luna MJ, et al. Identification of polypeptides in neurofibrillary tangles and total homogenates of brains with Alzheimer's disease by tandem mass spectrometry. J Alzheimers Dis 2013; 34: 239–62.
Miron J, Picard C, Labonte A, Auld D, Breitner J, Poirier J, et al. Association of PPP2R1A with Alzheimer's disease and specific cognitive domains. Neurobiol Aging 2019; 81: 234–43.
Montine TJ, Phelps CH, Beach TG, Bigio EH, Cairns NJ, Dickson DW, et al. National Institute on Aging-Alzheimer's Association guidelines for the neuropathologic assessment of Alzheimer's disease: a practical approach. Acta Neuropathol 2012; 123: 1–11.
Mori H, Kondo J, Ihara Y. Ubiquitin is a component of paired helical filaments in Alzheimer's disease. Science 1987; 235: 1641–4.
Myeku N, Clelland CL, Emrani S, Kukushkin NV, Yu WH, Goldberg AL, et al. Tau-driven 26S proteasome impairment and cognitive dysfunction can be prevented early in disease by activating cAMP-PKA signaling. Nat Med 2016; 22: 46–53.
Namba Y, Tomonaga M, Kawasaki H, Otomo E, Ikeda K. Apolipoprotein E immunoreactivity in cerebral amyloid deposits and neurofibrillary tangles in Alzheimer's disease and kuru plaque amyloid in Creutzfeldt-Jakob disease. Brain Res 1991; 541: 163–6.
Otvos L Jr, Feiner L, Lang E, Szendrei GI, Goedert M, Lee VM. Monoclonal antibody PHF-1 recognizes tau protein phosphorylated at serine residues 396 and 404. J Neurosci Res 1994; 39: 669–73.
Perry G, Friedman R, Shaw G, Chau V. Ubiquitin is detected in neurofibrillary tangles and senile plaque neurites of Alzheimer disease brains. Proc Natl Acad Sci USA 1987; 84: 3033–6.
Piras A, Collin L, Gruninger F, Graff C, Ronnback A. Autophagic and lysosomal defects in human tauopathies: analysis of post-mortem brain from patients with familial Alzheimer disease, corticobasal degeneration and progressive supranuclear palsy. Acta Neuropathol Commun 2016; 4: 22.
Pires G, McElligott S, Drusinsky S, Halliday G, Potier MC, Wisniewski T, et al. Secernin-1 is a novel phosphorylated tau binding protein that accumulates in Alzheimer's disease and not in other tauopathies. Acta Neuropathol Commun 2019; 7: 195.
Poppek D, Keck S, Ermak G, Jung T, Stolzing A, Ullrich O, et al. Phosphorylation inhibits turnover of the tau protein by the proteasome: influence of RCAN1 and oxidative stress. Biochem J 2006; 400: 511–20.
Sacco F, Perfetto L, Castagnoli L, Cesareni G. The human phosphatase interactome: an intricate family portrait. FEBS Lett 2012; 586: 2732–9.
Salminen A, Kaarniranta K, Haapasalo A, Hiltunen M, Soininen H, Alafuzoff I. Emerging role of p62/sequestosome-1 in the pathogenesis of Alzheimer's disease. Prog Neurobiol 2012; 96: 87–95.
Seyfried NT, Dammer EB, Swarup V, Nandakumar D, Duong DM, Yin L, et al. A multi-network approach identifies protein-specific co-expression in asymptomatic and symptomatic Alzheimer's disease. Cell Syst 2017; 4: 60–72.e4.
Sontag E, Nunbhakdi-Craig V, Lee G, Bloom GS, Mumby MC. Regulation of the phosphorylation state and microtubule-binding activity of Tau by protein phosphatase 2A. Neuron 1996; 17: 1201–7.
Sotiropoulos I, Galas MC, Silva JM, Skoulakis E, Wegmann S, Maina MB, et al. Atypical, non-standard functions of the microtubule associated Tau protein. Acta Neuropathol Commun 2017; 5: 91.
Spillantini MG, Goedert M. Tau pathology and neurodegeneration. Lancet Neurol 2013; 12: 609–22.
Szklarczyk D, Gable AL, Lyon D, Junge A, Wyder S, Huerta-Cepas J, et al. STRING v11: protein-protein association networks with increased coverage, supporting functional discovery in genome-wide experimental datasets. Nucleic Acids Res 2019; 47: D607–13.
Tan JM, Wong ES, Kirkpatrick DS, Pletnikova O, Ko HS, Tay SP, et al. Lysine 63-linked ubiquitination promotes the formation and autophagic clearance of protein inclusions associated with neurodegenerative diseases. Hum Mol Genet 2008; 17: 431–9.
Vickers JC, Riederer BM, Marugg RA, Buee-Scherrer V, Buee L, Delacourte A, et al. Alterations in neurofilament protein immunoreactivity in human hippocampal neurons related to normal aging and Alzheimer's disease. Neuroscience 1994; 62: 1–13.
Wang P, Joberty G, Buist A, Vanoosthuyse A, Stancu IC, Vasconcelos B, et al. Tau interactome mapping based identification of Otub1 as Tau deubiquitinase involved in accumulation of pathological Tau forms in vitro and in vivo. Acta Neuropathol 2017; 133: 731–49.
Wang Y, Martinez-Vicente M, Kruger U, Kaushik S, Wong E, Mandelkow EM, et al. Tau fragmentation, aggregation and clearance: the dual role of lysosomal processing. Hum Mol Genet 2009; 18: 4153–70.
Wang Q, Woltjer RL, Cimino PJ, Pan C, Montine KS, Zhang J, et al. Proteomic analysis of neurofibrillary tangles in Alzheimer disease identifies GAPDH as a detergent-insoluble paired helical filament tau binding protein. FASEB J 2005; 19: 869–71.
Wang Y, Zhang Y, Hu W, Xie S, Gong CX, Iqbal K, et al. Rapid alteration of protein phosphorylation during postmortem: implication in the study of protein phosphorylation. Sci Rep 2015; 5: 15709.
Wegmann S. Liquid-liquid phase separation of tau protein in neurobiology and pathology. Adv Exp Med Biol 2019; 1184: 341–57.
Xu L-R, Liu X-L, Chen J, Liang Y. Protein disulfide isomerase interacts with tau protein and inhibits its fibrillization. PLoS ONE 2013; 8: e76657. doi: 10.1371/journal.pone.0076657.
Xu J, Patassini S, Rustogi N, Riba-Garcia I, Hale BD, Phillips AM, et al. Regional protein expression in human Alzheimer's brain correlates with disease severity. Commun Biol 2019; 2: 43.
Yoshimura Y, Ichinose T, Yamauchi T. Phosphorylation of tau protein to sites found in Alzheimer's disease brain is catalyzed by Ca2+/calmodulin-dependent protein kinase II as demonstrated tandem mass spectrometry. Neuroscience Letters 2003; 353: 185–8.
Zhang Q, Ma C, Gearing M, Wang PG, Chin LS, Li L. Integrated proteomics and network analysis identifies protein hubs and network alterations in Alzheimer's disease. Acta Neuropathol Commun 2018; 6: 19.
Zhang Y, Sloan SA, Clarke LE, Caneda C, Plaza CA, Blumenthal PD, et al. Purification and characterization of progenitor and mature human astrocytes reveals transcriptional and functional differences with mouse. Neuron 2016; 89: 37–53.